Synthetic Assessment of the Centralized Voltage Control Impact on the Radial Network Operation

Synthetic Assessment of the Centralized Voltage Control Impact on the Radial Network Operation

Andrea Mazza
Dipartimento Energia "Galileo Ferraris"
Politecnico di Torino
Torino, Italy
andrea.mazza@polito.it

Gianfranco Chicco
Dipartimento Energia "Galileo Ferraris"
Politecnico di Torino
Torino, Italy
gianfranco.chicco@polito.it

***Abstract*— The analysis of the electrical distribution systems is typically carried out by considering multiple time steps and the corresponding variations of the load and generation. This is required especially in the case of non-negligible share of non-dispatchable and dispersed renewable energy sources (NDD-RES), which have a high impact on the node net power and hence on the current and voltage values, as well as on the energy losses. To improve the voltage profile, a deeper understanding is needed of the effects of the centralized voltage control and of new distributed solutions aimed to support the diffusion of NDD-RES. This paper is focused on the role of the centralized voltage control in the present context of deep NDD-RES penetration. The grid operation is characterized by different indicators based on the network voltages and currents, by investigating the conflicting nature among these indicators by taking the slack voltage magnitude as a parameter. The results show that the proper use of these indicators can drive the setting of the centralized voltage control during the different time steps, by including only values leading to the Pareto optimality based on the considered grid performance indicators.**

Keywords*— *Radial distribution system, Voltage variation, Energy Losses, Loading level, Pareto front, Slack voltage.

I. INTRODUCTION

The electrical distribution network operation is radial, with possible redundant branches to enable reconfiguration of the network in case of contingencies or to improve the network operational efficiency. In the presence of distributed energy resources, especially with non-dispatchable and dispersed renewable energy sources (NDD-RES), the voltage control of the distribution system needs to take into account both the centralized control applied at the starting point of the radial network and the local control depending on the control capabilities of the systems connected at the local nodes. In fact, the traditional voltage control used in the distribution systems without local generation was based on increasing the voltage at the supply point to avoid undervoltages in the terminal nodes of the radial network. However, in the presence of local generation it is possible to find overvoltages in some nodes of the network, so that a local voltage control has to complement the centralized voltage control in steady-state [1] and dynamic conditions [2].

The centralized voltage control is typically based on the on-load tap changer (OLTC) of the high-/medium-voltage (HV/MV) transformer and on shunt capacitor banks or static var compensators connected at the busbars of the MV supply node. For the distributed voltage control, besides typical solutions such as shunt capacitors and in some cases series voltage regulators along the feeders, more recently there has been a drastic increase of local voltage control from distributed generation (DG) with different electrical machines (from synchronous generators interfaced with transformers to generation units with direct current (DC) supply and power converter-based grid interfaces.

For the analysis of the electrical distribution systems, the variability of the load and DG during the day requires making calculations at multiple time steps. The traditional duration of the time steps used in for the assessment of the grid variables are 15 minutes, 30 minutes and one hour. Time steps with relatively low duration are more effective in understanding the changing power flows occuring in the network.

For the assessment of the distribution network operation, it is possible to determine different indicators that follow the evolution in time of the network voltages and currents. With these indicators, it is possible to quantify the effectiveness of the system operation and the possible occurrence of situations close to the operational limits of the network. These indicators include, for example, the deviations of the node voltage magnitude with respect to the voltage reference, the loading level of the branches, the energy losses in a given time period, the number (or cost) of the switching operations of the OLTC, as well as more specific entries such as the current sharing error referring to the current injections of DG into the grid [3].

The above-mentioned indicators refer to objectives that can be in conflict or not with each other. Two indicators are *conflicting* when the improvement of one of them implies the worsening of the other one. It is evident that the presence of conflicting indicators implies the unfeasibility of finding a unique optimal condition for both objectives. In that case, it is possible only to recognize a subset of sub-optimal conditions, representing the *non-dominated solutions* of the problem under analysis. A solution is *non-dominated* when no other solution exists with better values for all the individual indicators. The set of the non-dominated solutions forms the so-called *Pareto front*; the points forming the Pareto front are *compromise solutions*. The choice of the preferred solution requires the use of decision-making methods enabling to formalise the preferences of the decision maker and ranking the solutions accordingly. Fig. 1 shows four examples of Pareto fronts with different nature of the indicators to be maximised or minimised. The marked areas represent how to identify the solutions dominated by point A in the various cases. The orange dots indicate the Pareto front.

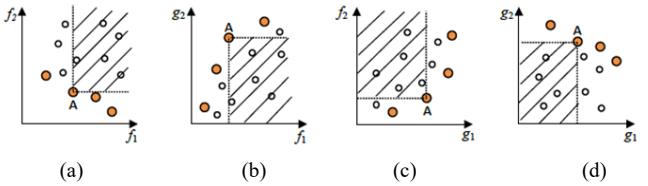

Fig. 1. Example of Pareto fronts: f_1 and f_2 have to be minimised, whereas g_1 and g_2 have to be maximised. (a) min-min case; (b) min-max case; (c) max-min case; (d) max-max case.

Table I shows an indicative (even though non-exhaustive) selection of papers that consider specific conflicting objectives. The energy losses and the voltage deviations with respect to the voltage reference are by far the preferred pair of conflicting objectives used in multi-objective problems referring to voltage control of distribution systems.

TABLE I. CONFLICTING OBJECTIVES CONSIDERED BY SOME LITERATURE CONTRIBUTIONS

	Energy losses	Voltage deviations	OLTC switching (# or cost)	Current sharing error
Mendoza *et al*., (2007) [4]	x	x		
Huiling *et al*., (2020) [5]	x	x		
Zhang *et al*., (2020) [6]	x	x		
Dong *et al*., (2018) [7]	x	x		
Kyrionidis *et al*., (2020) [8]	x		X	
Dissanayake and Ekneligoda (2020) [3]	x	x		x

The assessment of the possible conflicting solutions needs to consider a set of operational cases that differ with each other because of the setting of one or more decision parameters. A typical case is the calculation of the solutions obtained with the same load and generation, by testing different configurations of the network (i.e., with a different set of open branches such that the network remains radial). For a large distribution network with Medium Voltage (MV) and Low Voltage (LV) networks, the trade-off between the energy losses in the MV network and the total energy consumption (demand plus losses) in the LV system has been addressed in [9] in the context of conservative voltage reduction (that is, a reduction of the supply voltage to reduce the energy consumption of the users).

Taking two or more objective functions, the possible presence of conflicting solutions is not always clear-cut. Different situations may appear, in which pairs of objectives can be in conflict or not with each other depending on some operational conditions of the network.

This paper discusses the possible conflicts among different indicators by taking the slack voltage magnitude as the decision parameter. The variation of the voltage magnitude at the slack node is considered with the same load and generation, and represents the effect of the centralized control on the above-mentioned indicators.

It is shown that an indicator based on the voltage deviations with respect to a given reference may be either in conflict or not with the other indicators depending on the range of values of the slack voltage magnitude. This result also implies that the centralized control can be applied to obtain compromise solutions for the voltage deviations with respect to the energy losses and the loading level of the branches, provided that the slack voltage magnitude belongs to a range of voltages found through Pareto front analysis. This aspect is of interest, because it results from the analysis of the overall distribution system at a given time period. The same analysis can be repeated for different time periods with variable generation and load, finding out a synthetic way to determine the operational ranges of the slack voltage for centralized control, representing the complexity in time and space of the distribution system operation by looking only at the indicators that could represent conflicting solutions. This synthetic way is originally discussed in this paper, suppported by simulations carried out on a realistic test network.

The remainder of this paper is organized as follows. Section II introduces the network operation indicators used in the analysis. Section III shows and discusses the results obtained on the realistic test network. The last section contains the concluding remarks.

II. NETWORK OPERATION INDICATORS

In this paper, the network operation is described through three indicators, namely, the energy losses, the maximum deviation of the node voltage magnitude from the reference value (i.e., $V_{\text{ref}} = 1$ pu) and the maximum line loading level.

Let us consider the analysis of the grid behavior during a time period composed of T time steps of the same duration τ, expressed in hours. Moreover, let us suppose that the grid has N nodes and B branches, and indicate the node set as $\mathcal{N} \in \mathbb{N}^{N,1} = \{n \mid n = 1, \dots, N\}$ and the branch set as $\mathcal{B} \in \mathbb{N}^{B,1} = \{b \mid b = 1, \dots, B\}$.

The three network indicators are written as follows:

- *Energy losses*: by indicating with R_b the resistance of the branch b and with I_b the current flowing in the branch b, the energy losses over the entire analysis period are:

$$\mathcal{E}_{\text{loss}} = \tau \sum_{t=1}^{T} R_b I_b^2 \tag{1}$$

- *Voltage deviation*: over the entire time period under analysis, the voltage deviation is given by:

$$\Delta V_{\max} = \max_{t=1,\dots,T} \left\{ \left| V_{ref} - \max_{n \in \mathcal{N}} \{V_n(t)\} \right|, \left| V_{ref} - \min_{n \in \mathcal{N}} \{V_n(t)\} \right| \right\} \tag{2}$$

- *Line loading*: by indicating with $I_b^{(th)}$ the thermal limit of the branch b, the line loading, expressed in p.u., is:

$$\dot{I}_{max} = \max_{t=1,\dots,T;\ b \in \mathcal{B}} \left\{ \frac{I_b(t)}{I_b^{(th)}} \right\} \tag{3}$$

By considering these indicators as objectives, the construction of the Pareto front that contains the compromise solutions, enables the identification of the possible conflicting objectives. However, in general the conflicting nature of the objectives could be found only in a partial region of operation of the system. This aspect is not obvious, and is investigated with particular detail in the examples presented in this paper.

III. CASE STUDY

The case study refers to a rural network representative of a possible Italian distribution grid layout [10]. It is composed of 102 nodes (excluding the slack bus) and it is operated at 20 kV of nominal voltage, also used as the base voltage V_b in the per unit system. The base power has value $S_b = 1$ MVA. From these values, the base current is 28.9 A.

The structure of the grid is shown in Fig. 2. The grid includes DG (of photovoltaic type), which is connected at the light blue nodes, whereas the loads are all modelled as PQ nodes, with time-variant profiles depending on the load types (residential, industrial and agricultural loads, respectively).

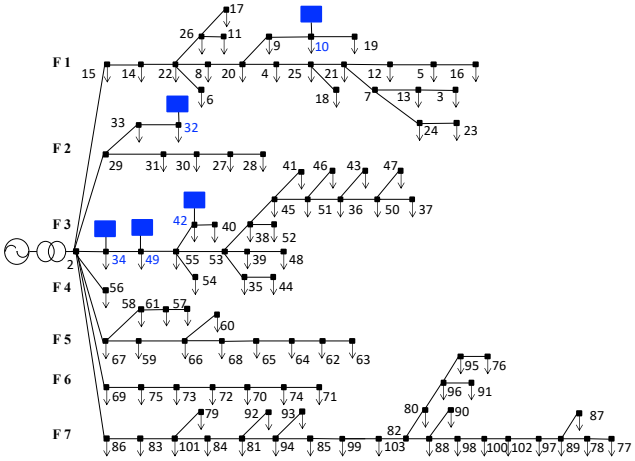

Fig. 2. Test network structure.

The loads are different in types and sizes, so that each node has a net active and reactive power patterns different with respect to the others. Fig. 3 shows some examples of load and generation patterns at time step of 15 minutes (i.e., $\tau = 0.25$ h).

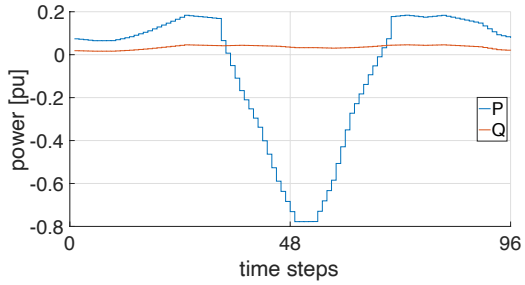

(a) Net power pattern at node 41 with load and DG.

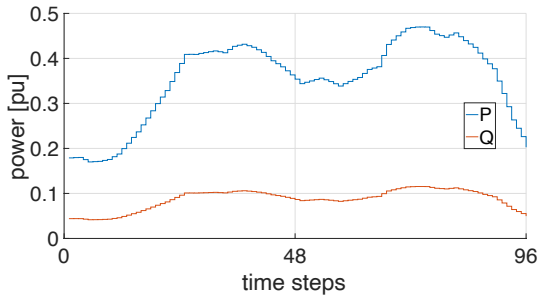

(b) Net power pattern at node 62 with load only.

Fig. 3. Examples of net power patterns at selected nodes.

A. Evaluation of the network indicators during the whole day

The power flow has been solved considering a time horizon of 24 hours with time step $\tau = 0.25$ h. The slack voltage has been varied in the range $0.9 \div 1.1$ (i.e., $0.9 \leq V_{slack} \leq 1.1$), with step 0.001. Totally, 201 simulations have been executed; however, part of these solutions cannot be used to build the Pareto front because of the constraint violation. In particular, in this example the violated constraint refers to the voltage value, whereas all the currents flowing in the branches lie within the admissible range.

First of all, it is necessary to understand whether the three network indicators are conflicting with each other or not. The absence of conflict between two indicators would permit considering only one of these indicators as the main indicator, disregarding the other indicator. As shown in Fig. 4, the energy losses and the loading level are not conflicting in the whole range of variation of the slack node voltage magnitude, whereas, as pointed out by Fig. 5 and Fig. 6, the voltage deviation is conflicting with both the loading level and the losses, even though the conflicting nature of the objectives occurs only for part of the operational conditions considered. For this reason, in the following analysis only the voltage deviation and the energy losses will be considered, neglecting the loading level.

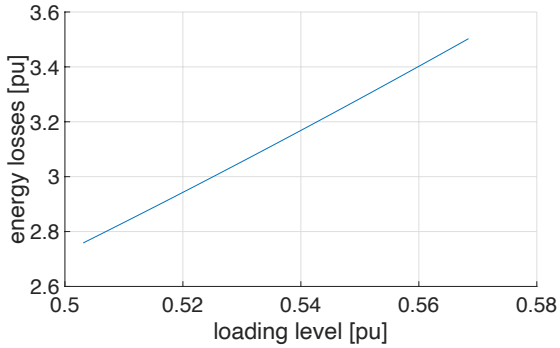

Fig. 4. Whole day: energy losses vs loading level.

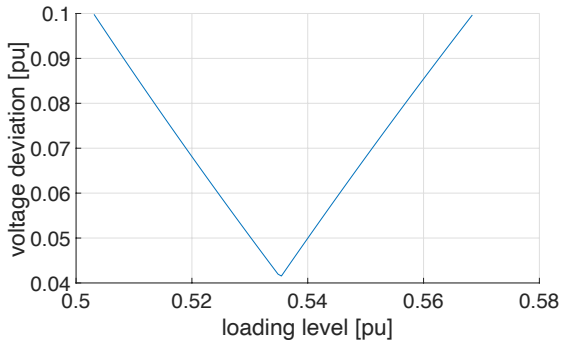

Fig. 5. Whole day: voltage deviation vs loading level.

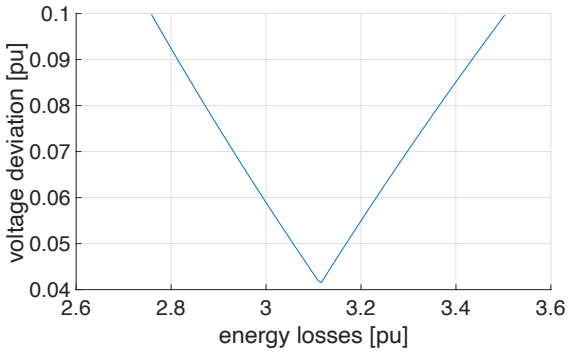

Fig. 6. Whole day: voltage deviation vs energy losses.

The number of simulations without any constraint violation is 113, corresponding to slack voltage values lying in the range $0.971 \leq V_{slack} \leq 1.083$.

By considering the values of the voltage deviation shown in Fig. 4, Fig. 5 and Fig. 6, it is worth to note that the maximum value is 10%, which is directly linked to the chosen

slack voltage maximum range (±10% of the nominal voltage).

The daily energy losses vary from about 2.75 p.u. to about 3.50 p.u., i.e., less than 1% of the total net load. This implies that the network is not particularly loaded, as proven by the maximum value of loading level that is less than 0.6 for the entire set of simulations.

By considering Fig. 5 and Fig. 6, it is possible to recognized the left-side branch as the Pareto front (since both indicators should be minimized). Among the 113 configurations without constraint violation, the configurations that compose the Pareto front are 60 and their slack value belongs to the range $1.024 \leq V_{slack} \leq 1.083$. The Pareto front is shown in Fig. 7 by considering the voltage deviation and the energy losses: the energy losses forming the Pareto front lie in the range $2.76 \leq \mathcal{E}_{\text{loss}} \leq 3.12$, whereas the loading level of the solutions forming the Pareto front ranges between 0.50 pu and 0.54 pu.

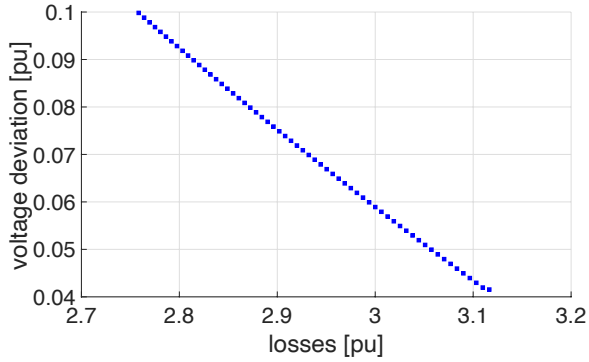

Fig. 7. Whole day: Pareto front of voltage deviation and energy losses.

B. *Evaluation of the network indicators during the daytime*

On the basis of the photovotaic generation, a subset of the time steps has been considered as daytime (range $33 \leq t \leq 69$). As a matter of example, only the relashionship between voltage deviation and energy losses is shown in Fig. 8. The shape is quite similar to the one reported in Fig. 6, but with different values of the losses, i.e., $1.08 \leq \mathcal{E}_{\text{loss}} \leq 1.41$. Moreover, the values of loading level differ with respect to the previous ones, lying in the range $0.45 \leq \dot{I}_{max} \leq 0.52$.

The number of cases without any constraint violations is larger than the one referring to whole day, being 125 over 201. Moreover, the slack voltage magnitude range is larger than in the previous case, i.e., $0.959 \leq V_{slack} \leq 1.083$: in fact, thanks to the presence of DG, it is possible also to operate the grid with lower slack voltage magnitude without any constraint violation.

Also in this case, the left-branch represents the Pareto front (shown in Fig. 8): it is composed of 65 points (over 125), with slack voltage magnitude range equal to $1.019 \leq V_{slack} \leq 1.083$. The energy losses lie in the range $1.08 \leq \mathcal{E}_{\text{loss}} \leq 1.23$, whereas the loading level range is $0.45 \leq \dot{I}_{max} \leq 0.48$.

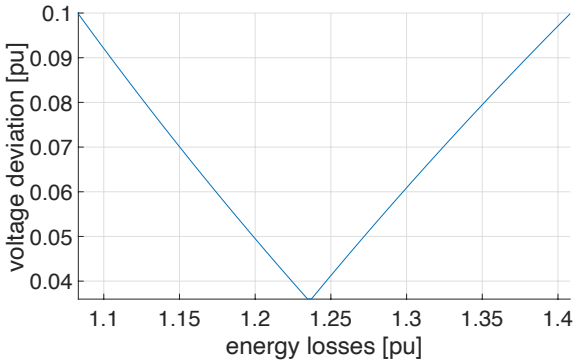

Fig. 8. Day-time: voltage deviation vs energy losses.

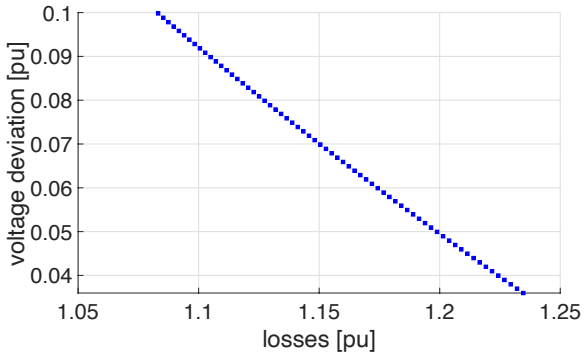

Fig. 9. Day-time: Pareto front of voltage deviation and energy losses.

C. *Evaluation of the network indicators during the night time*

The night time is the union of two disjoint subsets, i.e., $\forall\, t \mid \{1 \leq t \leq 32\} \cup \{70 \leq t \leq 96\}$, representing the time steps when there is no DG production. With reference to the grid operation for which there are no constraint violations, the number of solutions is 130 and the ranges of the the loading level values and the energy losses are $0.49 \leq \dot{I}_{max} \leq 0.57$ and $1.62 \leq \mathcal{E}_{\text{loss}} \leq 2.13$, respectively.

The values of the slack voltage for which the grid may be operated without any constraint violation lie in the range $0.97 \leq V_{slack} \leq 1.1$: as expected, the grid is completely passive, and hence the voltage drops along the feeder. For this reason, the network can be operated with higher slack voltage, with a slighly improvement on both the losses values and the loading level.

The Pareto front regarding the night time is shown in Fig. 10. The front is composed of 68 points, with voltage deviation and energy losses range equal to $0.49 \leq \dot{I}_{max} \leq 0.53$ and $1.62 \leq \mathcal{E}_{\text{loss}} \leq 1.86$, respectively.

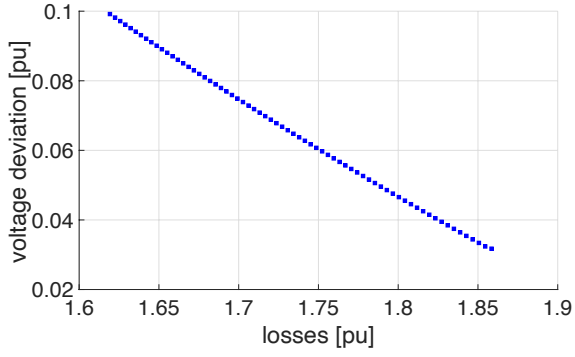

Fig. 10. Night-time: Pareto front of voltage deviation and energy losses.

D. *Evaluation of the 15-minute network indicators*

By considering all the single time steps, each of them can be characterized with its own Pareto front, as shown in Fig. 11. The number of points forming the Pareto fronts without violating the constraints change over time, as reported in Fig. 12.

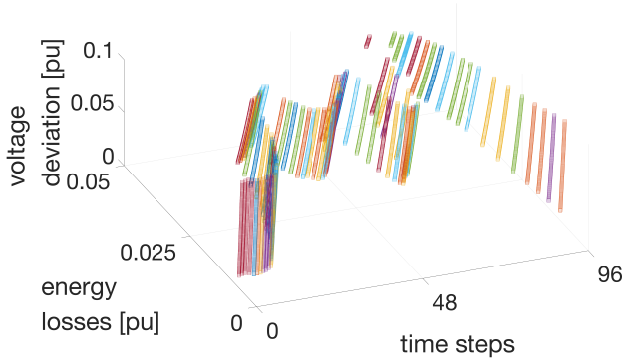

Fig. 11. 15-minute Pareto fronts of voltage deviation and energy losses.

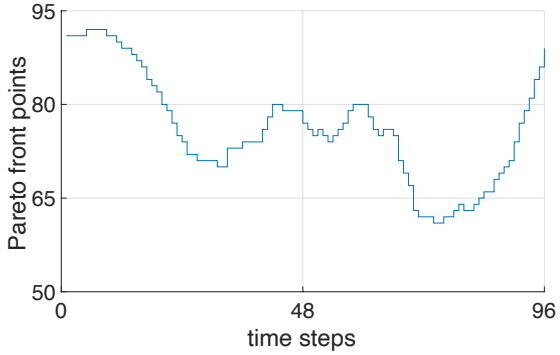

Fig. 12. Number of points of the 15-minute Pareto fronts.

Fig. 13 shows the slack voltage magnitude limits referring to the Pareto fronts. As expected, during the night the maximum voltage may even reach 1.1, whereas the presence of the DG it is possible to find the classical shape of the photovoltaic curve in the mid-day period. Regarding the minimum voltage, the values vary much more. In the presence of relative low load and no DG, the minimum voltage is around 1.01. Then, with a load increase and without significant photovoltaic generation (in closer to the sunrise and to the sunset), the minimum voltage is higher (about 1.04 pu). In presence of DG, in the day analysed the slack voltage magnitude is reduced to values close to the night ones (about 1.01 pu).

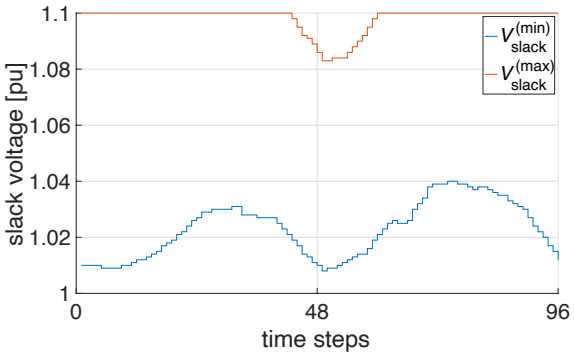

Fig. 13. Minimum and maximum slack voltage magnitude values with reference to the 15-minute Pareto fronts.

E. *Discussion on the generation and load models*

The power flow calculations have been carried out by considering a PQ node model at all the system nodes. This model can be considered to be realistic for the photovoltaic generation, for which the active power depends on the output referring to the solar irradiance and on the characteristics of the power conversion system at each time step, while the reactive power could be considered almost null because of the action of the control system at the grid interface. On the other side, for the loads the hypothesis of assigned power could introduce more approximations, as some grid components that contribute to the nodal load have a response to voltage variations that does not maintain the active and reactive power constant. In general, the load models can be represented with the classical ZIP model or with models with dependence on voltage represented through exponents (e.g., [11]). However, the determination of the components of the ZIP model with their shared participations, or of the exponents used to characterize the load aggregation is a challenging task that is being continuously explored [12] also in the presence of DG [13]. Thereby, in many cases the assigned power model is considered at each time step, especially justified to calculate the power flows in the network in a single solution when active and reactive power measurements are available at the node terminals [14].

For the study presented in this paper, however, the assumption of assigned power could be less justified when the slack voltage magnitude changes in a significant range. In fact, with the same power the current tends to be relatively high when the voltage decreases, and relatively low when the voltage increases, with respect to what could happen with the use of a ZIP or exponent-dependent model. Changing the values of the currents affects the calculation of the losses in the network branches and could have an impact on the energy losses determined as an objective function in the study, as well as on the allocation of the network losses to the nodes on the basis of established procedures [15]. Nevertheless, the general shape of the Pareto fronts is not expected to change qualitatively even by considering more refined load models.

IV. Concluding Remarks

This paper has introduced a different prospect to address the identification of centralised voltage control ranges in distribution networks with respect to the classical literature. The focus has been set to the interpretation of the results that can be obtained from classical power flow calculations carried out with variable slack voltage magnitude. In this respect, the proposed approach can be applied to any model of the distribution system, in particular, including any type of local voltage controls. The only variables to monitor are the ones that appear in the definition of the indicators considered (i.e., voltage and current magnitudes), in the different time steps (i.e., 15 minutes in our case study).

The results show that energy losses and voltage deviations with respect to the reference cannot be always considered as conflicting objectives. In fact, part of the feasible operating conditions appear to be (non-conflicting) dominated solutions and are by definition non-Pareto optimal. This implies that the slack voltage magnitudes causing the non-Pareto optimal solutions should be avoided to skip operational conditions with both high energy losses and high

voltage deviation. This condition rises in the presence of massive DG penetration, whereas does not appear in case of a passive network. Moreover, it is worth noting that the variation of voltage magnitude for the centralized control allowed to highlight the presence of the Pareto front. If any DG local controls are implemented, these controls may impact on the Pareto front composition. However, even in that case, the proposed methodology of analysis still remains valid. In fact, without loss of generality, the presence of different local control approaches is included in the power flow results, and hence the proposed analysis encompasses the explicit implementation of the distributed control system.

The results of this paper are also influenced by the load model chosen. In fact, considering the PQ model for the loads simplifies the relation between voltages and currents, which basically are inversely proportional, thanks to the fixed values of the power with respect to the voltage values. Future work will investigate the possible inclusion of a ZIP or exponent-dependent model of the loads, for evaluating the effectiveness of the above results, and the use of different grid layouts to investigate the effect of the network parameters on the determination of the centralized voltage control ranges.

The results of the analysis developed in this paper will be used to establish suitable centralized voltage control strategies, taking into account the characteristics of the voltage control systems available in the network. From these results, useful inputs are provided in a simple way, to understand possible ranges of variation of the slack node voltage magnitude in which there are conflicting solutions at different time steps. In fact, the solutions located onto the Pareto front provide viable ranges of voltage magnitudes, variable with time.

The proposed calculations do not provide directly the control signals to be used in coordinated voltage control among centralized and decentralized controllers. The specific contribution is to select the voltage magnitude ranges from which the voltage magnitude at the grid supply point can be set up at different time steps, for example as the voltage reference for the control systems used in the centralized equipment. These voltage references may be incorporated in more elaborated studies concerning voltage control coordination in distribution systems. Further work is in progress in this direction.

REFERENCES

[1] N. Jenkins, R. Allan, P. Crossley, D. Kirschen, and G. Strbac, *Embedded Generation*, The Institution of Engineering and Technology, London, UK, 2000.

[2] H.S. Bidgoli and T. Van Cutsem, "Combined Local and Centralized Voltage Control in Active Distribution Networks," IEEE Trans. on Power Systems, vol. 33, no. 2, pp. 1374-1384, 2018.

[3] A.M. Dissanayake and N.C. Ekneligoda, "Multiobjective Optimization of Droop-Controlled Distributed Generators in DC Microgrids," *IEEE Trans. on Industrial Informatics*, vol. 16, no. 4, pp. 2423-2435, 2020.

[4] J.E. Mendoza, D.A. Morales, R.A. Lopez, E.A. Lopez, J.C. Vannier, and C.A. Coello Coello, "Multiobjective Location of Automatic Voltage Regulators in a Radial Distribution Network Using a Micro Genetic Algorithm," *IEEE Trans. on Power Systems*, vol. 22, no. 1, pp. 404-412, 2007.

[5] T. Huiling, W. Jiekang, W. Fan, C. Lingmin, L. Zhijun, and Y. Haoran, "An Optimization Framework for Collaborative Control of Power Loss and Voltage in Distribution Systems with DGs and EVs Using Stochastic Fuzzy Chance Constrained Programming," *IEEE Access*, vol. 8, pp. 49013-49027, 2020.

[6] C. Zhang, Y. Xu, Z.Y. Dong, and R. Zhang, "Multi-Objective Adaptive Robust Voltage/VAR Control for High-PV Penetrated Distribution Networks," *IEEE Trans. on Smart Grid*, vol. 11, no. 6, pp. 5288-5300, 2020.

[7] P. Dong, L. Xu, Y. Lin, and M. Liu, "Multi-Objective Coordinated Control of Reactive Compensation Devices Among Multiple Substations," *IEEE Trans. on Power Systems*, vol. 33, no. 3, pp. 2395-2403, 2018.

[8] G.C. Kryonidis, C.S. Demoulias, and G.K. Papagiannis, "A Two-Stage Solution to the Bi-Objective Optimal Voltage Regulation Problem," *IEEE Trans. on Sustainable Energy*, vol. 11, no. 2, pp. 928-937, 2020.

[9] H. Gharavi, L.F. Ochoa, X. Liu, G. Paterson, B. Ingham, and S. McLoone, "CVR and Loss Optimization Through Active Voltage Management: A Trade-off Analysis," *IEEE Trans. on Power Delivery*, vol. 36, no. 6, pp. 3466-3476, Dec. 2021.

[10] F. Pilo, G. Pisano, S. Scalari, D. Dal Canto, A. Testa, R. Langella, R. Caldon, and R. Turri, "ATLANTIDE — Digital archive of the Italian electric distribution reference networks," *CIRED Workshop Integration of Renewables into the Distribution Grid*, 29-30 May 2012.

[11] EPRI, Load modelling for power flow and transient stability computer studies – LOADSYN Code User's Manual, EPRI EL-5003, vol. 3, January 1987.

[12] N. Sandoval, Y. Gong, and C.Y. Chung, "Three-Phase Second-Order Analytic Probabilistic Load Flow with Voltage-Dependent Load," *IEEE Trans. on Power Systems*, vol. 38, no. 1, pp. 229-241, 2023.

[13] D.Q. Hung, N. Mithulananthan, and K.Y. Lee, "Determining PV Penetration for Distribution Systems with Time-Varying Load Models," *IEEE Trans. on Power Systems*, vol. 29, no. 6, pp. 3048-3057, 2014.

[14] S.M.H. Rizvi, S.K. Sadanandan, and A.K. Srivastava, "Real-Time ZIP Load Parameter Tracking Using Sensitivity-Based Adaptive Window and Variable Elimination with Realistic Synchrophasor Data," *IEEE Trans. on Industry Applications*, vol. 57, no. 6, pp. 6525-6536, 2021.

[15] E. Carpaneto, G. Chicco and J. Sumaili Akilimali, "Characterization of the loss allocation techniques for radial systems with distributed generation," *Electric Power Systems Research*, vol. 78, no. 8, pp. 1396–1406, 2008.